Vol. 24 • No. 16 • April 24 • 2012

D10488

www.advmat.de

ADVANCED MATERIALS

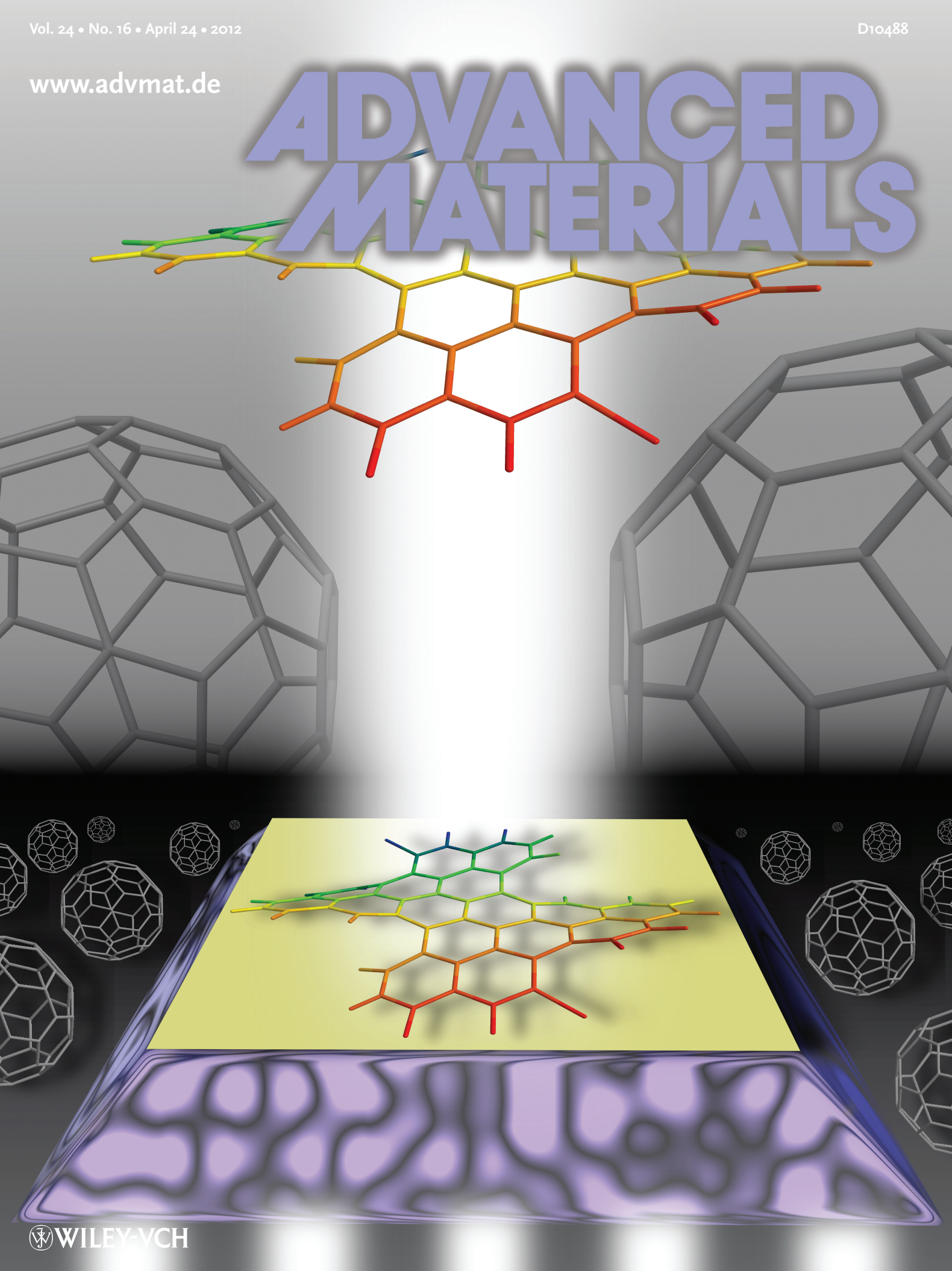

WILEY-VCH

Innovative Sensitizer DiPBI Outperforms PCBM

*Katharina Ditte, Wei Jiang, Thomas Schemme, Cornelia Denz, and Zhaohui Wang**

Holography has already led to an impressive variety of omnipresent and profitable applications. Worth mentioning is its usage in bank card, money bill, product security, supermarket scanners, as well as medical diagnostics. In addition to these inventions, the extension of holography to volume holography will certainly soon enrich our everyday-life through very promising implementations, as e.g., updateable 3-D displays, data storage devices,[1] and holographic projection in virtual reality. The most important step towards realization of these visionary approaches is the development of efficient multifunctional materials allowing adaptive and reversible holography as they are supplied by photorefractive (PR) materials. Photorefraction describes the reversible change of the refractive index during inhomogeneous illumination with light at very low light intensities. It requires photoconductivity and an electro-optic response. Inorganic PR crystals have been discovered in 1966,[2] elaborated specifically, and finally put into practical application in 2004 demonstrating optical storage of 10 Gb information in 1 cm^3.[3] However, up to now, the expensive production and the requirement of complex growth techniques for these crystals remain the main obstacle to commercialization. In order to circumvent these drawbacks, a considerable research effort has been directed towards replacement of inorganic materials by organic ones in the past 20 years. Based on this strategy, numerous organic, polymeric, and glassy PR materials have been designed, investigated, and proven to exhibit satisfying PR qualities.[4,5] The obvious advantages include low-cost synthesis, easy modification, and fast fabrication, at the same time requiring high electric fields for PR performance, and exhibiting a low sensitivity at low speed compared to their crystalline counterparts.

The challenge of organic PR materials preparation therefore still consists of combining molecules with photoelectric and electro-optic properties that are competitive with crystalline materials. Commonly this type of composites contain a polymeric hole transporter, a rod shape-like nonlinear optical (NLO) unit, and a sensitizer.[5] In these dc-field biased mixtures, the PR effect is observed when the following processes take place: The sensitizer absorbs optical radiation of a light pattern and thereby charge carriers are generated in the regions of high light intensity. Afterwards, while the sensitizer anions remain immobile, the mobile positive charge carriers are transported by the polymer to the dark regions, where they get trapped. This leads to the formation of a space-charge field E_{sc}, which rearranges the NLO molecules and thereby causes the refractive index change Δn. This induced index modulation is phase shifted with respect to the incident light pattern. According to the realignment of the NLO units in low glass-transition temperature materials, the refractive index change of the material is strongly affected by the orientational enhancement effect.[6]

The steady-state properties and the kinetics of PR materials can be probed with the technique of two-beam coupling (TBC).[7] The process is based on the interaction of two overlapping coherent laser beams with the simultaneously induced index modulation. The energy exchange between the beams which is expressed by the gain coefficient Γ depends not only on the amplitude of the space-charge field $|E_{sc}|$ but is strongly affected by the value of the phase shift ϑ between the index modulation and the interference pattern, see Equation (1)[7]

$$\Gamma \propto |E_{sc}| \sin(\vartheta) \tag{1}$$

Due to this unique phase-shift sensitivity, TBC provides the most significant evidence for photorefractive performance of a material.

Based on these physical mechanisms in polymeric composites the long-desired success has been reached by realizing updateable 3-D displays[8] and biomedical tomographs[9] using the well-known and widely used sensitizer [6,6]-phenyl-C61-butyric acid methyl ester (PCBM) (depicted in **Figure 1**). PCBM is a particularly favorable electron acceptor in donor/acceptor bulk heterojunction solar cells[10] and has been successfully applied as n-type material in OFETs[11] and photodetectors.[12] Nevertheless, applications as e.g. 3-D displays and biomedical tomographs need to be improved with respect to PR speed and light sensitivity in the operation, e.g. in the therapeutic window (600–1300 nm). Fortunately in both cases the underlying physical process is photoconductivity, which can be improved by the enhancement of the photocharge generation efficiency η and by the charge carrier mobility μ as explained by Equation (2).[13]

$$\sigma_{ph} \propto \eta\mu \tag{2}$$

Although a new hole transporting unit would increase the mobility and thereby the photoconductivity, the sensitivity of the PR material at a preferred wavelength and the PR speed can only be enhanced simultaneously by a high-performance charge generator. Therefore, in this contribution, highly absorbing sensitizers belonging to the class of perylene bisimide derivative are designed and synthesized for the first time to resolve this last challenge in applications in PR organic materials.

K. Ditte, T. Schemme, Prof. C. Denz
Institute of Applied Physics
Westfälische Wilhelms-Universität Münster
Corrensstr. 2, 48149 Münster, Germany
W. Jiang, Prof. Z. Wang
Institute of Chemistry
Chinese Academy of Sciences
Zhongguancun North First Street 2, 100190 Beijing, P. R. China
E-mail: wangzhaohui@iccas.ac.cn

DOI: 10.1002/adma.201104381

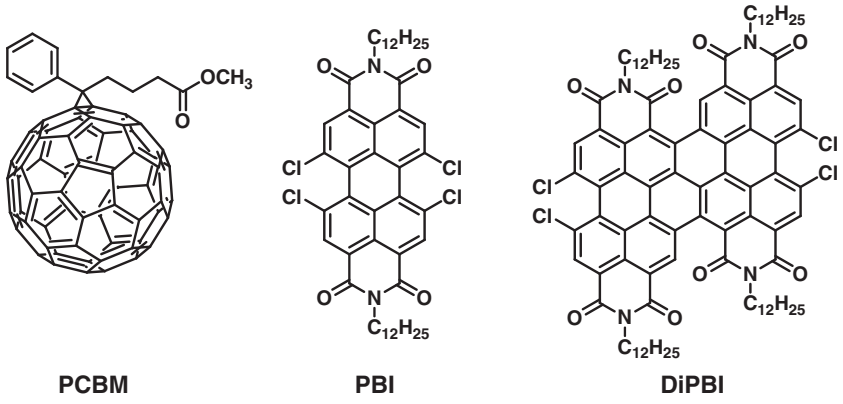

Figure 1. The molecular structures of PCBM, PBI, and DiPBI.

Perylene bisimide derivatives owing a large core of π-conjugated rings have been proven to provide many outstanding properties like strong absorption of visible light,[14] high fluorescence quantum yields,[15] and excellent photostability.[16] They demonstrate high electron affinity[17] and charge carrier mobility.[18] This large quantity of high-quality properties confirms the preferred usage of these molecules in the field of photo-voltaic cells,[19] organic field effect transistors (OFETs),[20] and organic light emitting diodes (OLEDs).[21] In order to establish these molecules in the area of nanoelectronics, graphene nanoribbons (GNRs), representing quasi-1D elongated strips of graphene nanostructures, were synthesized and characterized.[22] However, up to now, these promising features have not been exploited for improved PR materials. Among these omnipotent molecules is the novel sensitizer DiPBI which is a dimer of PBI. The molecular structures of these charge generators are shown in Figure 1.

The synthesis of DiPBI is conducted in optimized reaction condition according to a previous report.[23] These innovative dyes provide extraordinary thermal, chemical, and physical stability. Besides, PBI and DiPBI are highly soluble in common solvents like toluene, tetrahydrofurane, thiophene, and cyclohexanone.

In order to compare PCBM with the novel units PBI and DiPBI directly, the well investigated electro-optic mixture of the hole conductor poly-n-vinylcarbazole (PVK) and the liquid crystal 4-cyano-4-n-pentylbiphenyl (5CB)[24,25] is doped with the same molecular amount of the presented sensitizers. The compounds PVK, 5CB, and the sensitizer are dissolved in chloroform at the ratio 0.983:98.881:0.136 mol%. This ratio corresponds to 59.69:40.11:0.20 wt% (PVK:5CB:PCBM) (comparable to the effective composition used by Zhang and Singer),[25] 59.70:40.11:0.19 wt% (PVK:5CB:PBI), and 59.60:40.05:0.35 wt% (PVK:5CB:DiPBI) assuming PVK to be 37500 g mol^{-1} averaged. After this step the composite is dropped onto the ITO coated glass and annealed at 55 °C in an oven for 4 hours. Finally the composite is melt-pressed at 90 °C to the thickness of 50 µm defined by the spacer foil. The absorption spectra of the samples were measured by the spectrometer *Jasco V-530 UV/VIS* and are presented in **Figure 2**.

The influence of the sensitizers PCBM, PBI, and DiPBI on the absorption spectra is illustrated. The absorption of the sample containing DiPBI covers the whole range of visible light showing maxima in the blue, green, and red region. In contrast to this PBI absorbs blue and green light preferably. Hence, both sensitizers are particularly advantageous compared with the hardly absorbing PCBM.

Intending to prove that samples with a lower concentration of the novel sensitizers are remarkably effective, the dye amount of PBI and DiPBI has been decreased in the following samples, which were examined with the wavelength of 532 nm. The absorption coefficient α at 532 nm of the DiPBI samples is listed in **Table 1**.

The PR performance of the materials is investigated by two-beam coupling. The energy transfer between two beams in the PR samples is given by the gain coefficient Γ, which is depicted

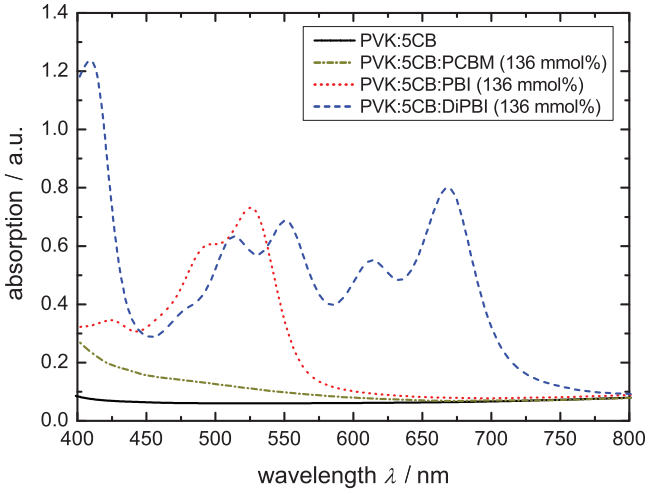

Figure 2. Absorption spectra of the unsensitized sample and samples doped with the same molecular amount of sensitizer.

Table 1. Absorption coefficient α, gain coefficient Γ, photoconductivity σ_{ph} ± 20%, internal photocurrent efficiency ϕ_{int} ± 20%, and PR speed for samples with varying DiPBI amount at 532 nm and E = 70 V µm^{-1}.

DiPBI amount [mmol%]	α [cm^{-1}]	Γ [cm^{-1}]	σ_{ph} [pS cm^{-1}]	ϕ_{int} [10^{-3}]	PR speed [s^{-1}]
136	56 ± 3	63 ± 6	0.64	0.23	5.9 ± 2.0
102	53 ± 2	49 ± 6	1.89	0.73	8.3 ± 2.0
68	41 ± 2	86 ± 7	1.01	0.50	10.0 ± 1.0
34	27 ± 1	188 ± 8	0.88	0.67	6.7 ± 0.5
17	16 ± 1	100 ± 9	0.28	0.35	2.6 ± 0.5
8.5	9 ± 1	94 ± 9	0.07	0.15	1.4 ± 0.5
4.25	6 ± 1	71 ± 6	0.01	0.042	0.7 ± 0.5

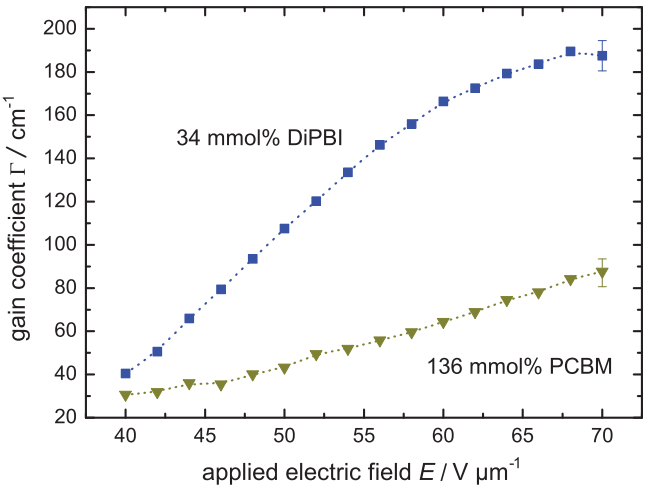

Figure 3. Gain coefficient Γ with respect to the applied electric field E for the samples with 136 mmol% PCBM and 34 mmol% DiPBI, respectively.

with respect to the applied electric field E in **Figure 3** for two samples containing 136 mmol% PCBM and 34 mmol% DiPBI, respectively. The values for the DiPBI sample are more than twice as high compared to the PCBM sample. The values for further DiPBI samples are given in Table 1. Note that in contrast to DiPBI, a decrease of the PCBM concentration in the composite leads to a decrease in photorefractivity.

The photoelectric qualities were measured with the picoammeter *6485 Keithley*, which are introduced in **Figure 4**(a). The behavior of the photoconductivity with respect to the sensitizer concentration reflects the contribution of the charge generation and mobility to the photoconductivity. The increase of the dye amount results in an increase of generated charge carriers and hence in a more pronounced photocurrent. But simultaneously with further increase of the dye percentage, the concentration of recombination centers in the composite accumulates and thus slows down the hole transport. That is why the mobility limit is reached in the samples with 136 mmol% of PBI and DiPBI.

The PR speed is the reciprocal value of the fast time constant achieved by fitting a biexponential decay function on the curves of the PR response. The slow time constant of the fit carried out can be attributed to the reorientation of the liquid crystal as a reaction on the light-induced space charge field, as no relation between the slow time constant and the internal photocurrent efficiency ϕ_{int} can be observed. The fast time constant in little doped DiPBI samples is strongly governed by the internal photocurrent efficiency. To elucidate the dependence of the PR speed on ϕ_{int} for DiPBI samples, the values for ϕ_{int} (calculated using Equation (4)) and the PR speed are given in Table 1. The influence of ϕ_{int} on the build-up of the space-charge field is as follows: The more charge carriers are generated, the higher is the space-charge field amplitude. Consequently, this can be considered as a rapider build-up of E_{sc}. For further examples compare the values of σ_{ph} with the ones of the PR speed depicted in Table 1. Note that values for the PCBM sample are: $\alpha = (9 \pm 1)$ cm^{-1}, $\sigma_{ph} = (0.021 \pm 0.004)$ pS cm^{-1}, $\phi_{int} = (0.048 \pm 0.009) \cdot 10^{-3}$, PR speed: (0.17 ± 0.02) s^{-1}, $\Gamma = (89 \pm 9)$ cm^{-1}.

Beside the influence of the sensitizer on the PR speed, the question of its effect on the NLO molecules and hence on the electro-optic response has remained unanswered until now. There were controversial indications in previous publications that the sensitizer anions hamper the alignment of the NLO units.[26,27] In order to resolve this issue, the birefringence of the material has been determined with respect to the sensitizer concentration via transmission ellipsometry. This technique reveals the difference between the extraordinary and the ordinary refractive index $|n_{eo} - n_o|$, which mirrors the poling order of the 5CB molecules.[28] In more detail, when the electric field is applied to the sample, an optical symmetry axis is induced in the composite resulting in an ordinary index n_o and an extraordinary index n_{eo} of refraction. Hence, the components of the electro-magnetic wave, perpendicular and parallel to the plane of incidence, experience different velocities in the poled material. Consequently a phase-shift between both polarization directions occurs resulting in a rotation of the light polarization behind the sample, see *Experimental*. The highest value of $|n_{eo} - n_o|$ of about $6.88 \cdot 10^{-3}$ is determined by the unsensitized composite, whereas the NLO performance descends with rising PBI and even stronger with DiPBI concentration reaching 4.67×10^{-3}, 3.35×10^{-3}, and 4.85×10^{-3} for samples with the same amount of PBI, DiPBI, and PCBM, respectively (see Figure 4(b)).

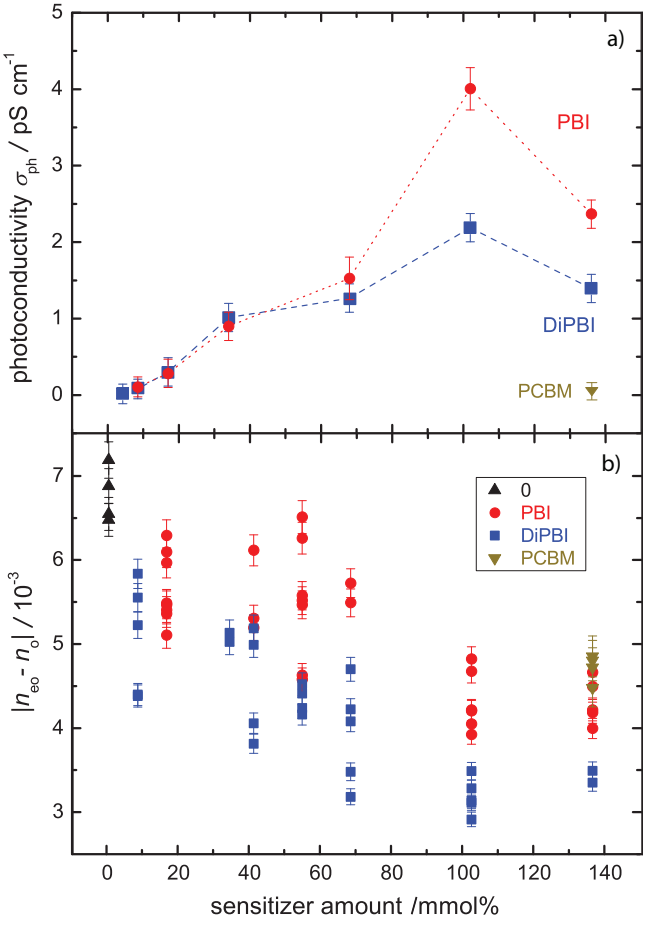

Figure 4. Photoconductivity σ_{ph} (a), birefringence $|n_{eo} - n_o|$ (b) at $E = 70$ V µm^{-1}.

Nevertheless, this behavior contradicts the assumption of disturbing charge generator anions, as the photocurrent in the PBI samples is known to be the highest, even 100 times higher than the one of the mixture containing PCBM. The correct explanation is as follows: In the sensitized composites the space is filled by the sensitizer, which was filled by 5CB molecules in the non-sensitized sample. As a result $|n_{eo} - n_o|$ decreases with rising charge generator concentration. Since PCBM and PBI have a comparable molecular weight, they are considered to fill the same volume per molecule and hence their composites show the same NLO properties. Moreover, DiPBI is a dimer of PBI and thus fills more space, which leads to an even lower birefringence.

Summarizing, a concentration dependent series of PR samples sensitized with PBI and novel DiPBI were prepared and compared with the PCBM doped one. The photoconductivity of the PCBM sample has not only been improved by a factor of 120 and 32 through the exchange of PCBM for PBI and DiPBI, respectively, but even the mobility limit has been reached. The increase of the PR speed for little concentrated DiPBI samples corresponds to the increase of the internal photocurrent efficiency. Thereby the DiPBI sample with only ¼ of PCBM amount showed a double PR gain and a 39 times faster PR speed. Furthermore, the photogenerated sensitizer anions were found out not to hamper the 5CB alignment. Thus, the innovative sensitizer DiPBI outperforms the widely used PCBM by far.

Experimental Section

Absorption coefficient: The absorption coefficient α was achieved measuring the intensity of the transmitted light of 532 nm behind the sample with a photodiode and relating these values to the one of the PCBM sample. The latter was measured with the help of the spectrometer *Jasco V-530 UV/VIS* and the Beer-Lambert law.

Photoconductivity: The picoammeter *6485 Keithley* was incorporated into the electric circuit to measure the dark current and the photocurrent produced with the wavelength of 532 nm with an intensity of 16 mW cm^{-2}. The electrode area $a = 39$ mm^2 and the thickness $d = 50$ µm of the samples were kept constant. The illumination of the samples took 110 seconds, after which the steady-state value of the photocurrent I_{ph} at the voltage U was used for the calculation of the photoconductivity σ_{ph} via equation

$$\sigma_{ph} = \frac{d\, I_{ph}}{a U} \tag{3}$$

The internal photoconductivity was achieved with the relation[29]

$$\phi_{int} = \frac{\sigma_{ph} E h\nu}{e \alpha d I} \tag{4}$$

where E is the applied electric field, h the Planck's constant, ν the light frequency, e the elementary charge, and I the light intensity.

Transmission ellipsometry: In order to quantify the phase shift $\Delta\phi_{sp}$, an under 45° linear polarized laser beam (intensity: 0.8 mW cm^{-2}) traversed the electro-optic medium. The light intensity I behind the polarizer is

$$I = I_0 \sin^2\left(\frac{\Delta\varphi_{sp}}{2}\right) \tag{5}$$

with I_0 being the intensity for parallel polarizers. This phase shift $\Delta\phi_{sp}$ depends on the wavelength λ, the optical path length L, and the birefringence, which can be obtained from

$$\left|\Delta\phi_{sp}\right| = \frac{2\pi L}{\lambda}\left|n_p - n_s\right| \tag{6}$$

In the 45° tilted sample configuration n_o coincides with n_s, while n_p has to be expressed using the approximation[26]

$$n_{eo} - n_o = \frac{n_p - n_s}{\sin^2(\theta)} \tag{7}$$

where θ is the angle of the laser beam inside the sample. The electric field was applied for 40 seconds.

Two-beam coupling: The energy exchange of the two p-polarized beams each with the intensity of 8 mW cm^{-2} was determined using the relation

$$\Gamma = \frac{1}{L}\left[\ln(\gamma b) - \ln(b + 1 - \gamma)\right] \tag{8}$$

with the gain $\gamma = I_1(I_2>0)/I_1(I_2 = 0)$ where $b = 1$ is the ratio between the intensities of the two interfering beams measured in front of the sample. The sample is tilted with respect to beam 1 by 40° and to beam 2 by 60° yielding a grating spacing of 2 µm assuming the refractive index to be 1.7. Field-dependent and sensitizer concentration-dependent measurements were carried out several times. The pre-illumination with only one beam and prepoling took 35 seconds before each measurement. The best value of the saturation after 50 seconds was used for the calculation of Γ.

Supporting Information

Supporting Information is available from the Wiley Online Library or from the author.

Received: November 15, 2011
Revised: January 26, 2012
Published online: March 26, 2012

[1] C. Denz, K. O. Muller, T. Heimann, T. Tschudi, *IEEE J. Sel. Top. Quantum Electron.* **1998**, *4*, 832.
[2] A. Ashkin, C. D. Boyd, M. Dziedzic, R. C. Smith, A. A. Ballman, J. J. Levinstein, K. Nassau, *Appl. Phys. Lett.* **1966**, *9*, 72.
[3] L. Cao, Q. He, H. Wei, G. Liu, C. Ouyang, J. Zhao, M. Wu, G. Jin, *Chinese Sci. Bull.* **2004**, *49*, 2429.
[4] W. E. Moerner, A. Grunnet-Jepsen, C. L. Thompson, *Annu. Rev. Mater. Sci.* **1997**, *27*, 585
[5] O. Ostroverkhova, W. E. Moerner, *Chem. Rev.* **2004**, *104*, 3267.
[6] W. E. Moerner, S. M. Silence, F. Hache, G. C. Bjorklund, *J. Opt. Soc. Am. B.* **1994**, *11*, 320.
[7] P. Yeh, *J. Quant. Electr.* **1989**, *25*, 484.
[8] P.-A. Blanche, A. Bablumian, R. Voorakaranam, C. Christenson, W. Lin, T. Gu, D. Flores, P. Wang, W.-Y. Hsieh, M. Kathaperumal, B. Rachwal, O. Siddiqui, J. Thomas, R. A. Norwood, M. Yamamoto, N. Peyghambarian, *Nature.* **2010**, *468*, 80.
[9] M. Salvador, J. Prauzner, S. Köber, K. Meerholz, J. J. Turek, K. Jeong, D. D. Nolte, *Opt. Express* **2009**, *17*, 11834.
[10] G. Yu, J. Gao, J. C. Hummelen, F. Wudi, A. J. Heeger, *Science.* **1995**, *270*, 1789.
[11] P. H. Wöbkenberg, D. D. C. Bradley, D. Kronholm, J. C. Hummelen, D. M. de Leeuw, M. Cölle, T. D. Anthopoulos, *Synt. Met.* **2008**, *158*, 468.
[12] D. Baierl, B. Fabel, P. Gabos, L. Pancheri, P. Lugli, G. Scarpa, *Org. Electron.* **2010**, *11*, 1199.
[13] D. Van Steenwinckel, E. Hendrickx, A. Persoons, *J. Chem. Phys.* **2001**, *114*, 9557.
[14] Y. Avlasevich, C. Li, K. Müllen, *J. Mater. Chem.* **2010**, *20*, 3814.
[15] T. Heek, C. Fasting, C. Rest, X. Zhang, F. Würthner, R. Haag, *Chem. Commun.* **2010**, *46*, 1884.
[16] Z. Tian, A. D. Shaller, A. D. Q. Li, *Chem. Commun.* **2009**, 180.
[17] H. Wang, H. Su, H. Qian, Z. Wang, X. Wang, A. Xia, *J. Phys. Chem. A.* **2010**, *114*, 9130.

[18] E. Di Donato, R. P. Fornari, S. Di Motta, Y. Li, Z. Wang, F. Negri, *J. Phys. Chem. B.* **2010**, *114*, 5327.
[19] A. P. H. J. Schenning, J. v. Herrikhuyzen, P. Jonkheijm, Z. Chen, F. Würthner, E. W. Meijer, *J. Am. Chem. Soc.* **2002**, *124*, 10252.
[20] S. Hüttner, M. Sommer, M. Thelakkat, *Appl. Phys. Lett.* **2008**, *92*, 093302.
[21] I. O. Balashova, J. Y. Mayorova, P. A. Troshin, R. N. Lyubovskaya, I. K. Yakushchenko, M. G. Kaplunov, *Mol. Cryst. Liq. Cryst.* **2007**, *467*, 295.
[22] Y. Zhen, C. Wanga, Z. Wang, *Chem. Commun.* **2010**, *46*, 1926.
[23] H. Qian, Z. Wang, W. Yue, D. Zhu, *J. Am. Chem. Soc.* **2007**, *129*, 10664.
[24] O. Ostroverkhova, K. D. Singer, *J. Appl. Phys.* **2002**, *92*, 1727.
[25] J. Zhang, K. D. Singer, *Appl. Phys. Lett.* **1998**, *72*, 2948.
[26] J. A. Quintana, P. G. Boj, J. M. Villalvilla, J. Ortiz, F. Fernandez-Lazaro, A. Sastre-Santos, M. A. Diaz-Garcia, *Appl. Phys. Lett.* **2005**, *87*, 261111.
[27] L. Martin-Gomis, F. Fernandez-Lazaro, A. Sastre-Santos, J. A. Quintana, J. M. Villalvilla, P. Boj, M. A. Diaz-Garcia, *Synthetic Metals.* **2007**, *157*, 1064.
[28] D. J. McGee, J. Y. Fukunaga, T. Zielinski, M. Yang, C. Salter, *J. Appl. Phys.* **2005**, *97*, 103102.
[29] T. K. Däubler, R. Bittner, K. Meerholz, V. Cimrova, D. Neher, *Phys. Rev. B.* **2000**, *61*, 13515.